

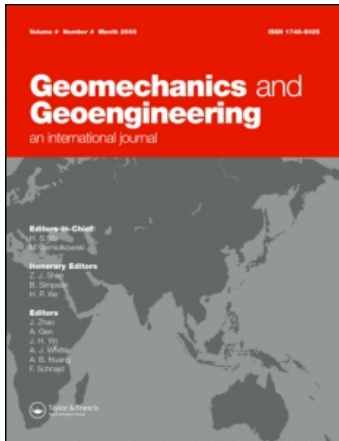
This article was downloaded by: [Canadian Research Knowledge Network]

On: 1 December 2010

Access details: Access Details: [subscription number 908883661]

Publisher Taylor & Francis

Informa Ltd Registered in England and Wales Registered Number: 1072954 Registered office: Mortimer House, 37-41 Mortimer Street, London W1T 3JH, UK



Geomechanics and Geoengineering

Publication details, including instructions for authors and subscription information:

<http://www.informaworld.com/smpp/title~content=t725304177>

An analytical solution for the nonlinear distribution of effective and total stresses in vertical backfilled stopes

Li Li^{abc}; Michel Aubertin^b

^a Genivar, Laval, Quebec, Canada ^b Department of Civil, Geological and Mining Engineering, École Polytechnique de Montréal, Montréal, Québec, Canada ^c Department of Construction Engineering, École de Technologie Supérieure, Montréal, Québec, Canada

Online publication date: 01 December 2010

To cite this Article Li, Li and Aubertin, Michel(2010) 'An analytical solution for the nonlinear distribution of effective and total stresses in vertical backfilled stopes', Geomechanics and Geoengineering, 5: 4, 237 – 245

To link to this Article: DOI: 10.1080/17486025.2010.497871

URL: <http://dx.doi.org/10.1080/17486025.2010.497871>

PLEASE SCROLL DOWN FOR ARTICLE

Full terms and conditions of use: <http://www.informaworld.com/terms-and-conditions-of-access.pdf>

This article may be used for research, teaching and private study purposes. Any substantial or systematic reproduction, re-distribution, re-selling, loan or sub-licensing, systematic supply or distribution in any form to anyone is expressly forbidden.

The publisher does not give any warranty express or implied or make any representation that the contents will be complete or accurate or up to date. The accuracy of any instructions, formulae and drug doses should be independently verified with primary sources. The publisher shall not be liable for any loss, actions, claims, proceedings, demand or costs or damages whatsoever or howsoever caused arising directly or indirectly in connection with or arising out of the use of this material.

An analytical solution for the nonlinear distribution of effective and total stresses in vertical backfilled stopes

Li Lj^{a,b,c} and Michel Aubertin^{b*}

^aGenivar, 2525 Boulevard Daniel Johnson, Suite 525, Laval, Quebec, Canada H7T 1S9; ^bDepartment of Civil, Geological and Mining Engineering, École Polytechnique de Montréal, C.P. 6079 succursale Centre-ville, Montréal, Québec, Canada H3C 3A7; ^cDepartment of Construction Engineering, École de Technologie Supérieure, 1100 Notre-Dame Ouest, Montréal, Québec, Canada H3C 1K3

(Received 30 July 2008; final version received 28 May 2010)

The increasing use of backfill in underground mines requires a proper evaluation of the stress state in and around the filled openings. This is, however, a relatively complex issue due, in part, to the large contrast in strength and stiffness between the backfill material and surrounding rock mass. In recent years, it has been shown that arching theory, based on limit equilibrium analysis, can be used to estimate the stress distribution in backfilled stopes. Nonetheless, many simplifications are involved in such analytical solutions and this affects the precision and significance of the calculated results. In this paper, a previously developed solution is enhanced by introducing the combined effects of non-uniform vertical stress distribution and positive pore water pressure. This leads to a more representative analytical solution, as demonstrated by successful comparisons with numerical simulations. The results indicate that the proposed solution can be used to estimate the effective and total stress state in submerged or partially submerged backfilled stopes with a simple geometry.

Keywords: backfill; mine stopes; total stresses; effective stresses; pore water pressure; arching effect

1. Introduction

Backfilling is playing an increasingly important role in the mining industry, as it can lead to an improvement in underground opening stability and to a significant reduction in the amount of mine wastes (when used as filling material) disposed on the surface. The growing use of backfill requires a good understanding of the stress state that develops in backfilled stopes. This is not a simple issue, in part because of the large contrast between the backfill strength and stiffness and those of the surrounding rock mass. For instance, a paste backfill containing 4.5% (w/w) of Portland cement typically shows a uniaxial compressive strength around 0.5 MPa and an elastic modulus of about 0.25 GPa (e.g., Belem *et al.* 2000); these values are 2 to 3 orders of magnitude lower than those measured on rocks. Hence, mine backfill is “soft” with respect to the mechanical behaviour of the surrounding rock mass. When backfill is put in a mined stope, it naturally settles under its own weight, while the stiff rock mass walls tend to hold the backfill in place. The settlement in the stope produces shearing along the rough surface walls. The shearing forces along the interfaces between the backfill and rock mass affect the stress state within the opening. The stress transfer to the abutments is particularly well developed in relatively narrow stopes, where it leads to a decrease in the vertical stress compared to

the overburden pressure (e.g., Aubertin 1999, Aubertin *et al.* 2003, Li *et al.* 2003, 2005). This stress transfer, which is often referred to as an “arching effect” (e.g., Handy 1985, Hunt 1986, Grice 1998, Pirapakaran and Sivakugan 2007b), has been confirmed by in-situ stress measurements (e.g., Knutsson 1981, Hustrulid *et al.* 1989, Belem *et al.* 2004) and by laboratory tests on physical models (e.g., Mitchell 1992, Pirapakaran and Sivakugan 2007a). It has been also confirmed by numerical simulations conducted by Li *et al.* (2003), who successfully compared the authors’ plane strain analytical solution with calculations performed with FLAC. The 2D solution of Aubertin *et al.* (2003) was later extended to 3D conditions by Li *et al.* (2005), while additional numerical simulations were conducted to investigate the effect of varying material properties and stope geometry (Li *et al.* 2007, Li and Aubertin 2009a). These solutions have also been used to evaluate the pressure acting on barricades located near the base of backfilled stopes (Li and Aubertin 2009d, 2009e).

Arching theory, originally developed by Janssen (1895), has been extensively used for silos and bins (e.g., Walker 1966, Cowin 1977, Blight 1986, Ooi and Rotter 1990, Drescher 1991). It was introduced in civil engineering by Marston (1930) to evaluate vertical loads on conduits placed in trenches (e.g., Spangler and Handy 1984, McCarthy 1988). Terzaghi (1943) also used a related approach to assess the stress state above horizontal openings (e.g., Ladanyi and Hoyaux 1969, Iglesias

*Corresponding author. Email: michel.aubertin@polymtl.ca

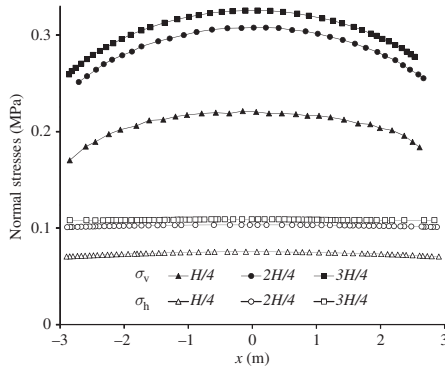


Figure 1. Numerical modelling results of the horizontal and vertical normal stress distribution across the width of a vertical (dry) backfilled stope (calculation results with single step backfilling, adapted from Li *et al.* 2003). The symbols are defined in Figure 2 and in the text; $H_b = H_m = 45$ m, $B = 3$ m; backfill properties: $E_b = 300$ MPa, $\mu_b = 0.2$, $\gamma_b = 18$ kN/m³, $\phi = 30^\circ$.

et al. 1999). Various other applications of arching theory have also been developed for different geotechnical structures such as retaining walls (Take and Valsangkar 2001, Goel and Patra 2008), and dams with confined cores (Kutzner 1997).

The specific solutions developed for stopes (and trenches) from arching theory are based on limit equilibrium analyses that involve a number of simplifying assumptions. For instance, most solutions assume that both the vertical and horizontal stresses are uniformly distributed across the width of the opening. Numerical calculations have indicated that this is not always a valid hypothesis, particularly for the vertical stress; this is illustrated in Figure 1, which shows simulation results on a typical filled opening (adapted from Li *et al.* 2003). An improved formulation has been recently proposed by Li and Aubertin (2008), who introduced a distribution factor (DF) to deal with the nonlinear vertical stresses. The latter solution does not, however, take into account the effect of pore water pressure. As water often plays an important role in the case of backfilled stopes, pore pressure should be included in the stress state calculations (Li and Aubertin 2009b,c).

In this paper, the analytical solution developed with a non-linear vertical stress distribution, proposed by Li and Aubertin (2008), is extended to include the effect of positive pore water pressure. The new 2D solution is presented in detail, and validated against numerical modeling results obtained for vertical backfilled stopes.

2. Equation formulation

Figure 2 schematically shows a vertical, narrow opening in which the backfilling material is (partially or fully) submerged. In this figure, H_b is the total height of the backfill, $2B$ is the opening width, and H_m is the thickness of the wet (or moist) backfill above the water table (where the pore water pressure $u_w = 0$). The key properties of the wet backfill are the internal

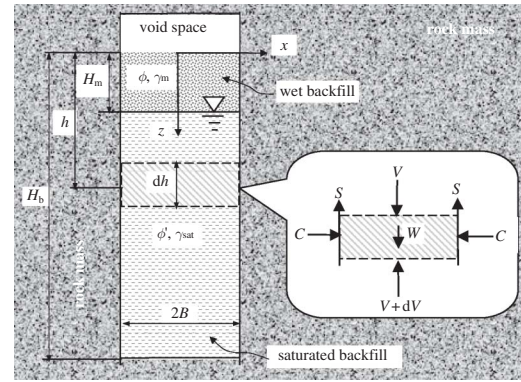


Figure 2. Schematic representation of a vertical backfilled stope with water table, showing the acting forces on an isolated layer element.

friction angle ϕ_m and unit weight γ_m , while those of the saturated backfill (below the water table) are the effective internal friction angle $\phi_{sat} (= \phi')$ and total unit weight γ_{sat} . The solution for the stress state in such openings can be obtained by solving the force summations for a series of element layers (e.g., Handy 1985, McCarthy 1988, Aubertin *et al.* 2003, Li *et al.* 2005).

Wet backfill

Considering a non-uniform vertical stress state above the water table ($h \leq H_m$), the solution proposed by Li and Aubertin (2008) is expressed as follows:

$$\sigma_{vx} = \sigma_{v0} \left\{ 1 - DF_m \left(\frac{|x|}{B} \right)^3 \right\} \quad (1)$$

where

$$\sigma_{v0} = \frac{\gamma_m B}{K_m \tan \delta_m} \left\{ 1 - \exp \left(- \frac{K_m \tan \delta_m}{B (1 - DF_m/4)} h \right) \right\} \quad (2)$$

The uniform horizontal stress then can be calculated from the following equation:

$$\sigma_h = K_m \sigma_{v0} \quad (3)$$

In the above equations, h is the depth from the backfill surface, x is the distance from the vertical center line ($-B \leq x \leq B$), σ_{vx} is the non-uniform (symmetric) vertical stress across the width of the opening, σ_{v0} is the vertical stress at the center line (at $x = 0$), δ_m is the friction angle at the interface between the backfill and rock mass, with $\delta_m \leq \phi_m$ (Li *et al.* 2003, 2005, Aubertin *et al.* 2005), and $K_m (= (1 - \sin \phi_m)/(1 + \sin \phi_m))$ is the active reaction coefficient. The non-linearity of the vertical stress across the width depends here on the distribution factor DF_m (Li and Aubertin 2008), which can be written as:

$$DF_m = \frac{2^{-\lambda}}{\tan^{0.1} (50^\circ + \phi_m)} \quad (4)$$

with

$$\lambda = 2 + \frac{H_b}{100B} \tag{5}$$

The distribution factor DF_m is used to represent the non-uniform normal vertical stress across the width (illustrated in the numerical result shown in Figure 1). When $DF_m = 0$, the stress becomes uniform (independent of x).

Saturated (submerged) backfill

The above solution is extended to obtain the stress state in the backfill below the water table ($h > H_m$), which can also be evaluated by considering a thin horizontal layer element subjected to its own weight W . In Figure 2, the forces on the element are the lateral compressive force C , the shearing force S , and the vertical forces V and $V + dV$. Equilibrium of the layer element below the water table requires that

$$dV + 2S = W \tag{6}$$

The weight of the backfill in this layer (for a unit thickness dh) is given by:

$$W = \gamma_{sat} 2B dh \tag{7}$$

Using the same development as for Equation (1), the effective vertical stress, σ_{vx}' , can be expressed as follows:

$$\sigma_{vx}' = \sigma_{v0}' \left\{ 1 - DF_{sat} \left(\frac{|x|}{B} \right)^3 \right\} \tag{8}$$

where σ_{v0}' is the effective vertical stress at the vertical center line of the slope ($x = 0$). DF_{sat} is the distribution factor in the saturated backfill, which can be written as:

$$DF_{sat} = \frac{2^{-\lambda}}{\tan^{0.1} (50^\circ + \phi_{sat})} \tag{9}$$

where λ is given by Equation (5).

The total vertical stress, σ_{vx} , is calculated as:

$$\sigma_{vx} = \sigma_{vx}' + u_w = \sigma_{vx}' + \gamma_w (h - H_m) \tag{10}$$

where u_w is the hydrostatic pore water pressure at equilibrium (only positive pore pressure is considered: $u_w \geq 0$), and γ_w is the unit weight of water.

To solve Equation (6), one needs to define the total vertical force acting on the layer element shown in Figure 2, which can be expressed as:

$$V = 2 \int_0^B \sigma_{vx} dx = 2B \left\{ \sigma_{v0}' (1 - DF_{sat}/4) + \gamma_w (h - H_m) \right\} \tag{11}$$

The ensuing shearing force S is estimated with the commonly used Mohr-Coulomb criterion:

$$S = \sigma_h' \tan \delta_{sat} dh = K_{sat} \sigma_{v0}' \tan \delta_{sat} dh \tag{12}$$

where σ_h' is the effective horizontal stress. The total horizontal stress is then given by

$$\sigma_h = \sigma_h' + u_w = K_{sat} \sigma_{v0}' + u_w \tag{13}$$

In Equations (12) and (13), K_{sat} is the active reaction coefficient for the saturated backfill:

$$K_{sat} = \sigma_h' / \sigma_{v0}' = \tan^2(45^\circ - \phi_{sat}/2) \tag{14}$$

(with $\phi_{sat} = \phi'$, the effective internal friction angle)

The submerged unit weight of the backfill is obtained from Equations (6), (7), (11) and (12):

$$\begin{aligned} \gamma_{sub} &= \gamma_{sat} - \gamma_w \\ &= (1 - DF_{sat}/4) \frac{d\sigma_{v0}'}{dh} + \frac{K_{sat} \tan \delta_{sat}}{B} \sigma_{v0}' \end{aligned} \tag{15}$$

Solving Equation (15) and considering the boundary condition at $h = H_m$, one obtains the effective vertical stresses at the vertical center line of the slope:

$$\begin{aligned} \sigma_{v0}' &= \frac{\gamma_{sub} B}{K_{sat} \tan \delta_{sat}} \left\{ 1 - \exp \left[\frac{K_{sat} (\langle H_m \rangle - h)}{B(1 - DF_{sat}/4)} \tan \delta_{sat} \right] \right\} \\ &+ \frac{\gamma_m B}{K_m \tan \delta_m} \left\{ 1 - \exp \left[- \frac{K_m \langle H_m \rangle}{B(1 - DF_m/4)} \tan \delta_m \right] \right\} \\ &\times \exp \left[\frac{K_{sat} (\langle H_m \rangle - h)}{B(1 - DF_{sat}/4)} \tan \delta_{sat} \right] \end{aligned} \tag{16}$$

where the MacCauley brackets are defined as $\langle H_m \rangle = (H_m + |H_m|)/2$.

The effective and total vertical stresses are thus obtained from Equations (8) and (10), while the total and effective horizontal stresses are calculated with Equations (13) and (14).

3. Representation of the stress distribution

The solution proposed above can be used to calculate the stress state in vertical backfilled stopes, for a variety of situations. For instance, Figure 3 shows the distribution of the total and effective stresses for different fill friction angles ϕ ($= \phi_m = \phi_{sat}$). These results have been obtained for a stope having a width of 6 m ($B = 3$ m), and a backfill height H_b of 50 m (with $H_m = 5$ m). The unit weight of the wet backfill $\gamma_m = 19$ kN/m³ and that of the saturated backfill $\gamma_{sat} = 20$ kN/m³.

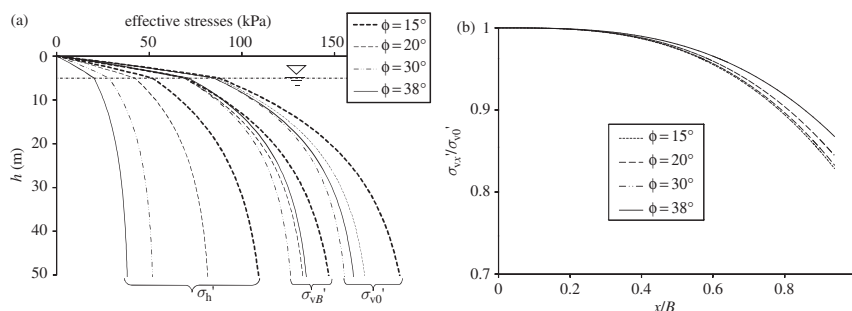


Figure 3. Variation of effective stresses (a) with elevation h calculated with the proposed solution with different fill friction angle ($\phi = \phi_m = \phi_{sat} = \phi'$); the phreatic surface is at $H_m = 5$ m, with $B = 3$ m, and $H_b = 50$ m; wet backfill: $\gamma_m = 19$ kN/m³; saturated backfill: $\gamma_{sat} = 20$ kN/m³; effective horizontal stress (σ_h') and vertical stresses at the vertical center line (σ_{v0}') and near the walls (σ_{vB}'); (b) effective vertical stresses across the width of the slope (σ_{vx}') normalized by the effective vertical stress at the vertical center line (σ_{v0}').

The calculation results shown in Figure 3 indicate that the effective stresses tend to decrease with an increase of the internal friction angle ϕ . The observed change of slope at the water table level for the effective stress distribution represents the effect of water pressure (Figure 3a). It is observed that the effective vertical stresses decrease with an increase of ϕ when its value is below about 30°, while the tendency is reversed for σ_{v0}' and σ_{vB}' when ϕ exceeds this value. This phenomenon has also been reported in previous investigations performed by the authors, following numerical calculations (Li and Aubertin 2009a,c). Figure 3a also shows that the effective vertical stress is smaller near the walls (σ_{vB}') than at the center of the slope (σ_{v0}'), with a difference that increases with depth h . This tendency is also illustrated in Figure 3b, which shows the effective vertical stress distribution (σ_{vx}') at mid-height of the slope, normalized by the effective vertical stress at the center (σ_{v0}'). It is seen in this figure that the effective vertical stress decreases progressively from the center and reaches its minimum value at the wall ($x = B$). The non-uniformity (curvature) of the σ_{vx}' distribution tends to decrease slightly with an increase of the friction angle ϕ .

Figure 4 shows the influence of slope width (B) on the effective stress distribution. Again, a slope change is observed in the stress profile at the water table level, indicating a decrease of the effective stress with an increase of pore pressure. The effective stress also decreases with a decrease of slope width B . When the slope is very narrow (i.e. $B \leq 2$ m approximately in

this case), the effective stresses become almost constant with depth, as seen in Figure 4a. This figure also shows that the effective vertical stress is always smaller near the walls (σ_{vx}') than at the center (σ_{v0}') of the slope. This pattern is further confirmed by Figure 4b, which indicates that the non-uniformity of the vertical stress distribution σ_{vx}' tends to decrease somewhat with a reduction of the slope width B (for the geometry studied here).

A comparison between Figures 4 and 5 shows that the total stresses are significantly higher than the effective stresses. Figure 5 also indicates that the total stresses given by the proposed solution can be much smaller than those estimated from the total overburden weight of the backfill. The difference is related to the arching effect associated with the stress transfer to the rock mass.

4. Comparison with numerical modeling results

The basic arching solution developed for a dry backfill has been validated by comparing the calculated stresses with experimental data taken from the literature (Li *et al.* 2005). The analytical solution has also been compared with numerical simulation results to further validate the proposed formulation (Li *et al.* 2003, 2005). In the absence of experimental data for the vertical stresses in submerged backfill, only the latter validation procedure is applied here.

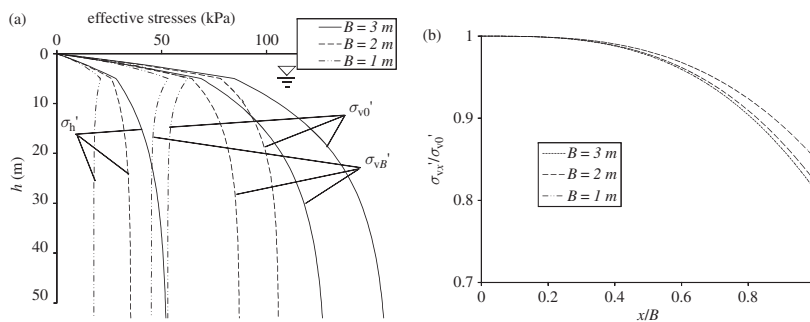


Figure 4. Influence of slope width B on the effective stresses along depth h (a) and width x (b); calculations made with $H_m = 4$ m, $H_b = 50$ m; wet backfill: $\phi_m = 30^\circ$, $\gamma_m = 19$ kN/m³; saturated backfill: $\phi_{sat} = 30^\circ$, $\gamma_{sat} = 20$ kN/m³.

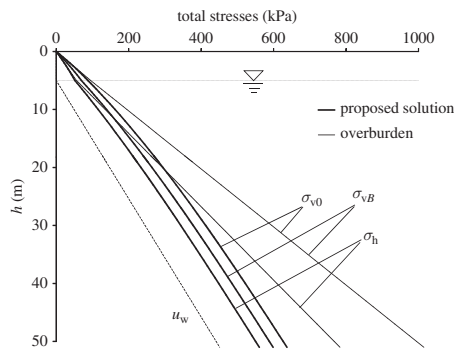


Figure 5. Total stresses calculated with the proposed solution; calculation made with $H_m = 4$ m, $H_b = 50$ m; wet backfill: $\phi_m = 15^\circ$, $\gamma_m = 19$ kN/m³; saturated backfill: $\phi_{sat} = 15^\circ$, $\gamma_{sat} = 20$ kN/m³.

Stress distributions calculated with the proposed analytical solution presented above are compared with numerical modeling results obtained with FLAC (Itasca 2002). The modeling procedure has been described by Li *et al.* (2003, 2009a). The configuration given in Figure 2 is used, with $B = 3$ m and $H_b = 45$ m. A typical discretization mesh is shown in Figure 6, with the boundary conditions and symmetry axis. The rock mass is linearly elastic, while the fill is modeled as a nonlinear elastoplastic Mohr-Coulomb material. The rock mass properties are: $E_r = 30$ GPa (Young's modulus), $\mu_r = 0.3$ (Poisson's ratio), $\gamma_r = 27$ kN/m³ (unit weight), and those of the backfill are: $E_b = 300$ MPa, $\mu_b = 0.2$, $c_b = 0$ (cohesion) and $\psi_b = 0^\circ$ (dilatation angle; non-associated flow rule). The simulation sequence considers that the slope is first mined. Backfilling

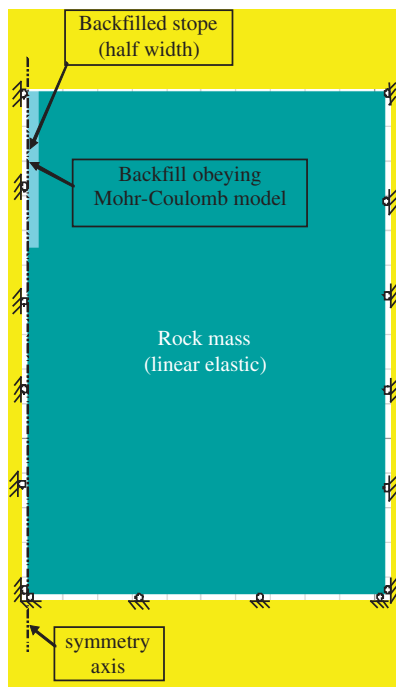


Figure 6. Discretization of the problem domain in FLAC with imposed boundary conditions.

of the opening begins after the release of elastic strains along the rock mass walls. Here, the addition of backfill is simulated in 15 steps to control the effect of non-static loading in FLAC (each step corresponds to one fill layer); additional filling steps (or layers) would not significantly change the calculated stresses (e.g., Pirapakaran and Sivakugan 2007b, Li and Aubertin 2009a).

Two sample cases are presented here:

- i) Partially submerged backfill. The water table is located 4 m below the backfill surface ($H_m = 4$ m in Figure 2); the backfill above the water table is characterized by $\gamma_m = 18$ kN/m³ and $\phi_m = 30^\circ$; for the saturated backfill (under water), $\gamma_{sat} = 20$ kN/m³ and $\phi_{sat} = \phi' = 30^\circ$.
- ii) Backfill under water. The backfill surface is located 4.36 m below the water table ($H_m = -4.36$ m in Figure 2); for the saturated backfill, $\gamma_{sat} = 20$ kN/m³ and $\phi_{sat} = \phi' = 30^\circ$.

Figures 7–9 show comparisons between the effective stresses and total stresses obtained from the proposed analytical solution (Case i) and from numerical simulations, along the vertical center-line (Figure 7), near the wall (Figure 8), and across the width of the slope at $h = 20$ m (Figure 9). The stresses shown in Figure 8 are taken at a small distance (a few cm) from the wall (within the backfill) to avoid the abrupt localized changes observed for σ_{vx}' and σ_{vx} (in the detailed results) due to the large difference in stiffness between the backfill and rock mass. Effective and total stresses based on overburden weight are also plotted in Figures 7 and 8. It is seen that the effective and total stresses calculated with the analytical solution (Equation (16) with Equations (8), (10), (13), and (14) for submerged backfill and Equations (1)–(3) for moist backfill) are well correlated with those obtained from the numerical simulations. The stress distributions again show a transition at the water table elevation. The results also show that the stresses calculated using the overburden weight tend to be overestimated when compared to those obtained from the numerical and analytical solutions, particularly at larger depth.

These results appear to indicate that the analytical solution, based on arching theory, correctly represents the stress distribution and load transfer to the abutment surrounding the backfill.

For fully submerged backfill (Case ii), comparisons between the analytical solution (Equation (16) with Equations (8), (10), (13), and (14)) and numerical results are shown along the vertical center-line (Figure 10), near the wall (Figure 11), and across the width of the slope at $h = 26$ m (Figure 12). Again, the agreement between the numerical and analytical solutions is quite good. The results also show that the total and effective stresses would be overestimated at depth by using the overburden weight.

For these sample cases (and for others not shown here), the stresses calculated with the proposed analytical solution and with FLAC are well correlated. The normal vertical and horizontal stresses are close to those based on the overburden weight at shallow depth in the backfill, where the effect of

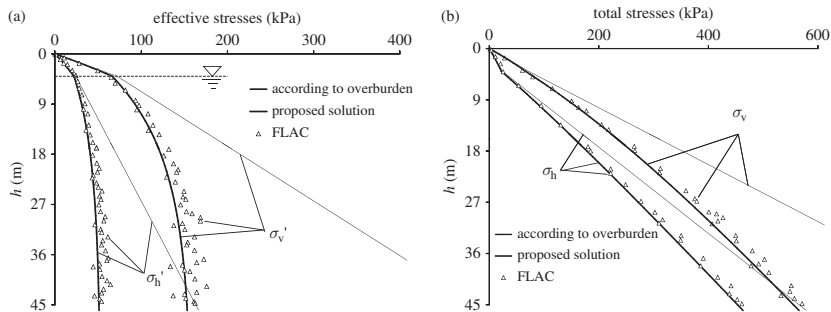


Figure 7. Vertical and horizontal effective (a) and total (b) stresses along the vertical center line, obtained from numerical modeling and the analytical solution (Case i).

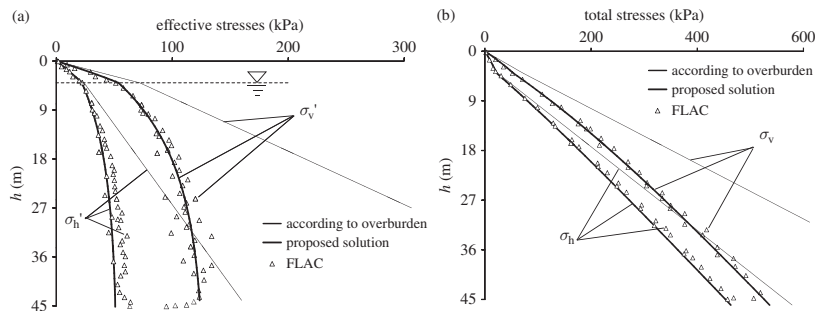


Figure 8. Vertical and horizontal effective (a) and total (b) stresses near the walls, obtained from numerical modeling and the analytical solution (Case i).

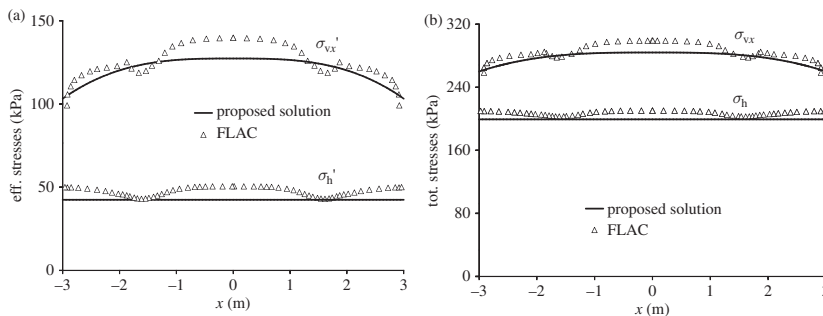


Figure 9. Vertical and horizontal effective (a) and total (b) stresses across the width of the slope, obtained from numerical modeling (Case i).

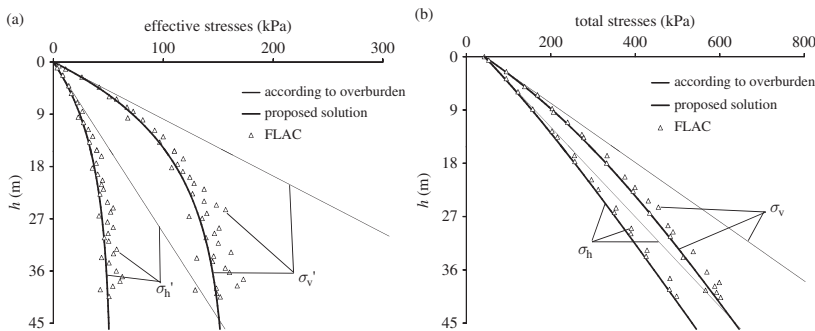


Figure 10. Vertical and horizontal effective (a) and total (b) stresses along the vertical center line, obtained from numerical modeling and the analytical solution (Case ii).

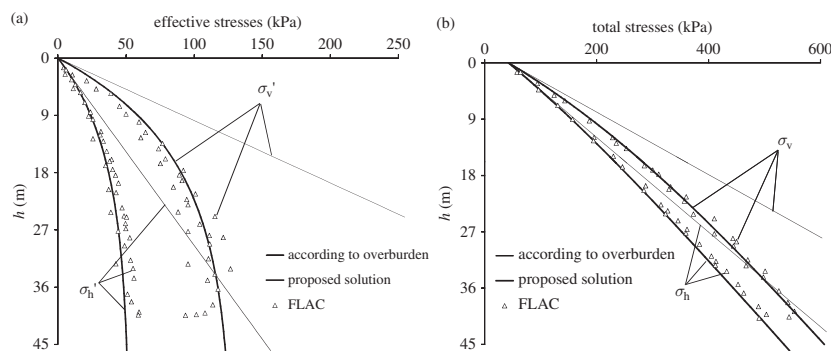


Figure 11. Vertical and horizontal effective (a) and total (b) stresses near the walls, obtained from numerical modeling and the analytical solution (Case ii).

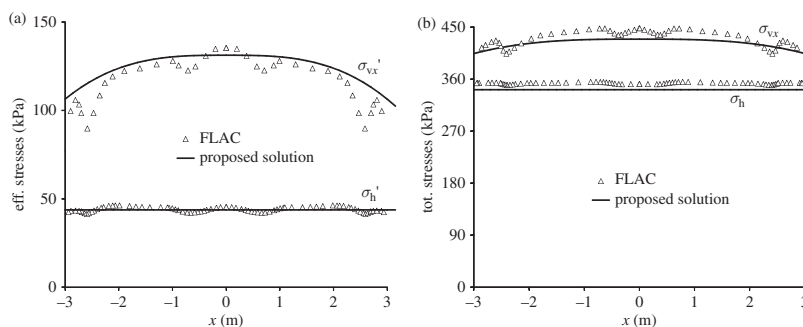


Figure 12. Vertical and horizontal effective (a) and total (b) stresses across the width of the stope, obtained from numerical simulations and the analytical solution (Case ii).

arching is negligible, while the stresses at larger depth tend to be reduced by the stress redistribution to the stiff walls surrounding the opening.

5. Discussion

The use of the proposed analytical solution can be quite convenient for simple applications, and can help reveal the particular behavior of backfilled stopes. For instance, when the opening is very narrow, calculations indicate that both the vertical and horizontal effective stresses may become almost constant with depth (Figure 4a). This response is also observed in numerical simulations (Li and Aubertin 2009a). Such type of behavior may be important for narrow vein mines and for small openings filled with broken rock and other cohesionless material. This example highlights the usefulness of such analytical solutions to assess the behavior of backfilled openings, at least in the early stages of a project.

It should nonetheless be recalled that the solution presented in this paper was developed by considering a 2D geometry (i.e. plane strain condition). In some cases, 3D conditions need to be taken into account. For such instances, the 3D analytical solutions developed by the authors can be used (e.g., Li *et al.* 2005, Li and Aubertin 2009b). However, the effect of the distribution factor DF has not yet been included in this solution (i.e. uniform vertical stresses are assumed across the stope width).

Another limitation of the proposed solution relates to the use of the Mohr-Coulomb criterion. This linear yield function may not always be appropriate when dealing with porous media, so another type of criterion may sometimes be preferable. More realistic models are being considered in additional investigations.

Other factors neglected here may also need to be taken into account when making a detailed analysis of backfilled stopes. These include the cohesion of the fill material, inclination of the stope, drainage and consolidation (with non-equilibrium pore pressure), progressive strength gain due to cementation, and effect of negative pore pressure (under unsaturated conditions). These additional features are addressed in complementary studies being conducted by the authors and their collaborators.

6. Conclusion

In this paper, existing analytical solutions based on arching theory are modified to obtain the effective and total stresses within vertical backfilled stopes under plane strain conditions. The modified solution takes into account the effect of positive pore pressure and of the non-uniform vertical stress distribution across the stope width. The solution proposed here indicates that the presence of water tends to significantly reduce the effective stresses below the water table, while the total stress is increased by the water pressure. The observed arching effect implies that both the effective and total stresses can be much

lower than the overburden pressure. In general, the horizontal (effective and total) stresses are quite uniform across the width of a stope, while the vertical stresses are higher at the center than along the wall at the same depth. This feature is well captured in the proposed solution. The good agreement between results obtained from the analytical solution and numerical simulations indicates that the proposed solution can be used to estimate the effective and total stresses within vertical backfilled openings.

Acknowledgements

The authors acknowledge the financial support from the Institut de Recherche Robert-Sauvé en Santé et en Sécurité du Travail du Québec (IRSST) and from the participants of the Industrial NSERC Polytechnique-UQAT Chair in Environment and Mine Wastes Management (<http://www.polymtl.ca/enviro-geremi/>). The authors thank Dr John Molson for his review of the manuscript.

References

- Aubertin, M., 1999. Application of soil mechanics to analyze the behaviour of underground backfill (in French). Short Course (unpublished), *14e Colloque en Contrôle de Terrain*, 23–24 March 1999, Val-d'Or, Qc. Quebec Mining Association.
- Aubertin, M., Li, L., Arnoldi, S., Belem, T., Bussière, B., Benzaazoua, M. and Simon, R., 2003. Interaction between backfill and rock mass in narrow stopes. In: P.J. Culligan, H.H. Einstein, and A.J. Whittle, eds. *Soil and Rock America 2003*. Essen: Verlag Glückauf, 1, 1157–1164.
- Aubertin, M., Li, L., Belem, T., Simon, R., Harvey, A., James, M., Benzaazoua, M. and Bussière, B., 2005. Methods to estimate induced pressures in backfilled stopes (in French). In: *Symposium Rouyn-Noranda: Mines and the Environment*, May 2005, Rouyn-Noranda, Canada. CIM, CD-ROM.
- Belem, T., Benzaazoua, M. and Bussière, B., 2000. Mechanical behaviour of cemented paste backfill. In: *Proceedings of the 53th Canadian Geotechnical Conference*, 15–18 October 2000, Montréal, 1, 373–380.
- Belem, T., Harvey, A., Simon, R. and Aubertin, M., 2004. Measurement and prediction of internal stresses in an underground opening due to backfilling with cemented paste. In: *Proc. 15th International Symposium on Ground Support in Mining and Underground Construction: Ground Support 2004*, 28–30 September 2004, Perth, Western Australia.
- Blight, G.E., 1986. Pressure exerted by materials stored in silos. Part I: coarse materials. *Géotechniques*, 36 (1), 33–46.
- Cowin, S.C., 1977. The theory of static loads in bins. *Journal of Applied Mechanics*, 44, 409–412.
- Drescher, A., 1991. *Analytical methods in bin-load analysis*. New York: Elsevier.
- Goel, S. and Patra, N.R., 2008. Effect of arching on active earth pressure for rigid retaining walls considering translation mode. *International Journal of Geomechanics ASCE*, 8 (2), 123–133.
- Grice, T., 1998. Stability of hydraulic backfill barricades. In: M. Bloss, ed. *MineFill'98: Proceedings of the 6th International Symposium on Mining and Backfill*, Brisbane, Australia, AusIMM, 117–120.
- Handy, R.L. 1985. The arch in soil arching. *Journal of Geotechnical Engineering ASCE*, 111 (3), 302–318.
- Hunt, R.E., 1986. *Geotechnical engineering analysis and evaluation*. New York: McGraw-Hill.
- Hustrulid, W., Qianyan, Y. and Krauland, N., 1989. Modeling of cut-and-fill mining systems – Näsleden revisited. In: F.P. Hassani, M.J. Scoble and T.R. Yu, eds. *Innovation in mining backfill technology*. Rotterdam: Balkema, 147–164.
- Iglesia, G.R., Einstein, H.H. and Whitman, R.V. 1999. Determination of vertical loading on underground structures based on an arching evolution concept. In: C. Fernandez and R.A. Bauer, eds. *Geo-Engineering for Underground Facilities*. Geo-Institute of ASCE, 495–506.
- Itasca, 2002. *FLAC – Fast Lagrangian Analysis of Continua, User's Guide*. Minneapolis: Itasca Consulting Group, Inc.
- Janssen, H.A., 1895. Versuche über Getreidedruck in Silozellen. *Zeitschrift Verein Ingenieure*, 39, 1045–1049.
- Kutzner, C., 1997. *Earth and rockfill dams: principles of design and construction*. Rotterdam: Balkema.
- Knutsson, S., 1981. Stresses in the hydraulic backfill from analytical calculations and in-situ measurements. In: O. Stephansson and M.J. Jones, eds. *Proceedings of Conference on Application of Rock Mech. to Cut and Fill Mining*, Institution of Mining and Metallurgy, London, 261–268.
- Ladanyi, B. and Hoyaux, B., 1969. A study of the trap-door problem in a granular mass. *Canadian Geotechnical Journal*, 6 (1), 1–14.
- Li, L. and Aubertin, M., 2008. An improved analytical solution to estimate the stress state in sub-vertical backfilled stopes. *Canadian Geotechnical Journal*, 45(10), 1487–1496.
- Li, L. and Aubertin, M., 2009a. A numerical investigation of the stress state in inclined backfilled stopes. *International Journal of Geomechanics ASCE*, 9(2), 52–62.
- Li, L. and Aubertin, M., 2009b. A three-dimensional analysis of the total and effective stresses in submerged backfilled stopes. *Geotechnical and Geological Engineering*, 27 (4), 559–569.
- Li, L. and Aubertin, M., 2009c. Influence of water pressure on the stress state in stopes with cohesionless backfill. *Geotechnical and Geological Engineering*, 27 (1), 1–11.
- Li, L. and Aubertin, M., 2009d. Horizontal pressure on barricades for backfilled stopes. Part I: Fully drained conditions. *Canadian Geotechnical Journal*, 46 (1), 37–46.
- Li, L. and Aubertin, M., 2009e. Horizontal pressure on barricades for backfilled stopes. Part II: Submerged conditions. *Canadian Geotechnical Journal*, 46 (1), 47–56.
- Li, L., Aubertin, M., Simon, R., Bussière, B. and Belem, T., 2003. Modeling arching effects in narrow backfilled stopes with FLAC. In: R. Brummer, P. Andrieux, C. Detournay and R. Hart, eds. *FLAC and Numerical Modeling in Geomechanics – 2003*. Rotterdam: Balkema, 211–219.
- Li, L., Aubertin, M. and Belem, T., 2005. Formulation of a three-dimensional analytical solution to evaluate stress in backfilled vertical narrow openings. *Canadian Geotechnical Journal*, 42 (6), 1705–1717 (with Erratum 43(3), 338–339).
- Li, L., Aubertin, M., Shirazi, A., Belem, T. and Simon, R., 2007. Stress distribution in inclined backfilled stopes. In: *Proceedings of the 9th International Symposium in Mining with Backfill*, April 29–May 2, 2007, Montreal, Quebec, Canada. CIM, CD-ROM.
- Marston, A., 1930. The theory of external loads on closed conduits in the light of latest experiments. Bulletin No. 96, *Iowa Engineering Experiment Station*, Ames, Iowa.
- McCarthy, D.F., 1988. *Essentials of soil mechanics and foundations: basic geotechnics*. Mahwah, NJ: Prentice Hall.

- Mitchell, R.J., 1992. Centrifuge model studies of fill pressures on temporary bulkheads. *CIM Bulletin*, 85 (960), 48–54.
- Ooi, J.Y. and Rotter, J.M., 1990. Wall pressures in squat steel silos from simple finite element analysis. *Computations and Structures*, 37 (4), 361–374.
- Pirapakaran, K. and Sivakugan, N., 2007a. A laboratory model to study arching within a hydraulic fill stope. *Geotechnical Testing Journal*, 30 (6), 1–8.
- Pirapakaran, K. and Sivakugan, N., 2007b. Arching within hydraulic fill stopes. *Geotechnical and Geological Engineering*, 25 (1), 25–35.
- Spangler, M.G. and Handy, R.L., 1984. *Soil engineering*. New York: Harper and Row.
- Take, W.A. and Valsangkar, A.J., 2001. Earth pressures on unyielding retaining walls of narrow backfill width. *Canadian Geotechnical Journal*, 38, 1220–1230.
- Terzaghi, K., 1943. *Theoretical soil mechanics*. New York: John Wiley & Sons.
- Walker, D.M., 1966. Approximate theory for pressures and arching in hoppers. *Chemical Engineering Science*, 21 (11), 975–997.